ChemComm

Accepted Manuscript

This article can be cited before page numbers have been issued, to do this please use: C. Gu, P. Gai, L. Han, W. Yu, Q. Liu and F. Li, *Chem. Commun.*, 2018, DOI: 10.1039/C8CC02328J.

ROYAL SOCIETY OF CHEMISTRY

rsc.li/chemcomm

View Article Online
DOI: 10.1039/C8CC02328J

Journal Name

COMMUNICATION

Enzymatic Biofuel Cell-Based Self-Powered Biosensing of Protein Kinase Activity and Inhibition via Thiophosphorylation-Mediated Interface Engineering†

Received 00th January 20xx,
Accepted 00th January 20xx

DOI: 10.1039/x0xx00000x

www.rsc.org/

Chengcheng Gu[‡a], Panpan Gai[‡a], Lei Han[a], Wen Yu[a], Qingyun Liu[b] and Feng Li*[a]

We developed a facile and ultrasensitive enzymatic biofuel cell (EBFC)-based self-powered biosensing of protein kinase A (PKA) activity and inhibition via thiophosphorylation-mediated interface engineering. The detection limit was down to 0.00022 U mL^{-1} (S/N = 3). In addition, the PKA activities from MCF-7 and A549 cell lysates were analyzed and achieved reliable results.

Enzymatic biofuel cell (EBFC)-based self-powered biosensing has been regarded as a facile and promising strategy which integrates the power supply device and biosensing instrumentation into the whole just with two electrodes[1-3]. Owing to the unique merits of no need for external power sources, simple instrumentation, miniaturization and excellent anti-interference ability[2, 3], the EBFC-based self-powered strategy has been widely applied in biomolecular assay[4-6], food security[7, 8], immunoassays[9], drug release[10], cytosensing[11, 12], and neurochemical sensing[13]. Among them, a series of effective approaches have been explored[2, 3, 14], including substrate effects[4], inhibition effects[6, 15], blocking effects[12, 16], and gene regulation effects[17, 18]. However, the deficiency of elaborated design on the interface of the biocathode and/or the bioanode makes the detected targets limited. Thus, in order to expand their practical applications and to take full advantages of the prominent features of the self-powered biosensors, the development of new design concepts is of great significance and challenge.

As we know, protein kinase-catalyzed phosphorylation plays a critical role in a majority of biological processes, including cell signal transduction, metabolism, cell growth, proliferation and apoptosis[19-21]. In these processes, phosphate groups can be transferred from adenosine-triphosphate (ATP) to amino acids in peptides or proteins *via* protein kinase catalysis[19]. What's more, the protein phosphorylation states and kinase activity are closely associated with many serious diseases, such as multifarious cancers and Alzheimer's diseases[22]. As a consequence, it is very essential to develop rapid and sensitive assays for precisely monitoring either protein kinase activity or their potential inhibitors, which is of great significance to the fundamental biochemical research[23], as well as the protein kinase-targeted drug discovery and molecular-target therapies[24]. Until now, various protocols have been utilized to determine the activity of protein kinase, including electrochemiluminescence[25, 26], surface-plasma resonance[27, 28], mass spectrometry[29, 30], fluorescence[31-33], electrochemistry[23, 34-38], photoelectrochemistry[39, 40], etc, in which, the design generally focused on the coordinative interaction between signal probe and phosphorylated peptide, and obtained excellent results. However, most of them required sophisticated instrumentation and complicated operations. Accordingly, attempts to exploit simple and effective strategy are urgently needed.

Herein, we developed a simple and ultrasensitive EBFC-based self-powered biosensing of PKA activity and inhibition via the ingenious design of thiophosphorylation-mediated interface. As shown in Scheme 1, the self-powered biosensing platform was composed of the glucose dehydrogenase (GDH)/CNT bioanode and the peptides/AuNPs biocathode. The negatively charged SiO_2@Au nanoparticles (SiO_2@AuNPs) would be captured by the biocathode through Au-S bond, only when the serine of the peptides on biocathode surface underwent thiophosphorylated process in the presence of target PKA with the assistance of adenosine 5'-[*γ*-thio] triphosphate (ATP-s). In this case, the electron transfer of the electron acceptor $[Fe(CN)_6]^{3-}$ at the biocathode surface would be obstructed due to the steric hindrance effects and electrostatic repulsion of SiO_2@AuNPs. Consequently, the open circuit voltage of EBFC (E^{OCV}) dramatically decreased,

[a] College of Chemistry and Pharmaceutical Sciences, Qingdao Agricultural University, Qingdao 266109, P. R. China.
[b] College of Chemical and Environmental Engineering, Shandong University of Science and Technology, Qingdao 266510, P. R. China.
‡ C. C. Gu & P. P. Gai contributed equally to this work.

†Electronic Supplementary Information (ESI) available: [Experimental section. Optimization of experimental conditions; DPV signal of the biocathode with different PKA and PKA inhibition concentrations; Comparison of analytical performance for PKA assay; Measurement of PKA in cell lysates]. See DOI: 10.1039/x0xx00000x

View Article Online
DOI: 10.1039/C8CC02328J

realizing the determination of PKA. Apart from the detection of PKA, the as-proposed EBFC-based self-powered biosensing platform also showed excellent performance for quantitative kinase inhibitor screening. Therefore, this facile and ultrasensitive self-powered biosensor showed great potential in protein kinases-related clinical diagnosis and drug discovery.

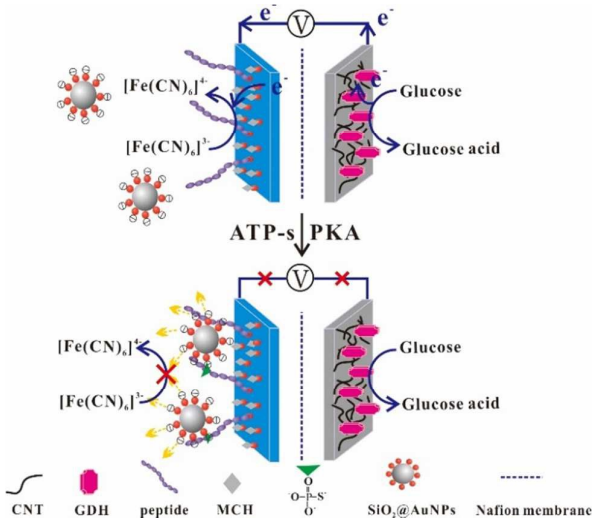

Scheme 1. Schematic Illustration of the Principle of the EBFC-Based Self-Powered Biosensing Strategy for PKA Analysis.

The key design of this proposed self-powered biosenor was the interface engineering of the biocathode (Scheme S1). Herein, AuNPs and the peptide chain CLRRASLG were selected as the biocathode substrate and the recognition sites of PKA (RRASL), respectively. The hydroxyl group of serine residue (S) could be replaced by γ-phosphoryl from ATP-s under the catalysis of PKA. In addition, cysteine-terminated peptides (C) could be immobilized on the AuNPs modified ITO electrode through the Au-S bond. Then it was treated with 6-mercapto-1-hexanol (MCH) to remove nonspecific adsorption sites. Once in the presence of the target PKA, it would firstly catalyze the peptide thiophosphorylated with the assistance of ATP-s. As such, the obstruction, *i.e.* the negatively SiO_2@AuNPs composite, could decorate on the modified electrode surface under the drive of Au-S action. The steric hindrance effects and electrostatic repulsion of SiO_2@AuNPs composite prevented $[Fe(CN)_6]^{3-}$ approaching to the biocathode, thus the electrochemical signal of the biocathode significantly decreased. While without PKA (even in the presence of ATP-s), the large-sized SiO_2@AuNPs could not be adsorbed on the electrode surface because of the lack of the thiophosphorylated active site. In this case, the reduction of $[Fe(CN)_6]^{3-}$ could easily occur and obtained a large current.

To verify the aforementioned processes, a series of experimental measurements were carried out. First, from the transmission electron microscopy (TEM) images in Fig 1A-C, the uniform structure of AuNPs ensured the efficient immobilization of the peptide through the Au-S bond. Meanwhile, AuNPs was also uniformly decorated on the SiO_2 surface. Noticeably, the diameter of SiO_2@AuNPs composite was about 200 nm, which could generate significant steric hindrance effects. Furthermore, to confirm the preparation of SiO_2@AuNPs and the effect of the electrostatic repulsion, the zeta potentials of different particles were examined (Fig. 1d). Initially, the bare SiO_2 spheres exhibited the zeta potential of -26.1 mV, and it could change to 30.3 mV after amino-functionalization. After the amino-functionalized SiO_2 surface was modified by the AuNPs (zeta potentials of -39.89 mV), the zeta potential decreased to -14.9 mV. All the above data strongly confirmed that the successful assembly of the negatively charged SiO_2@AuNPs composite, which could be well applied in the biocathode interface engineering.

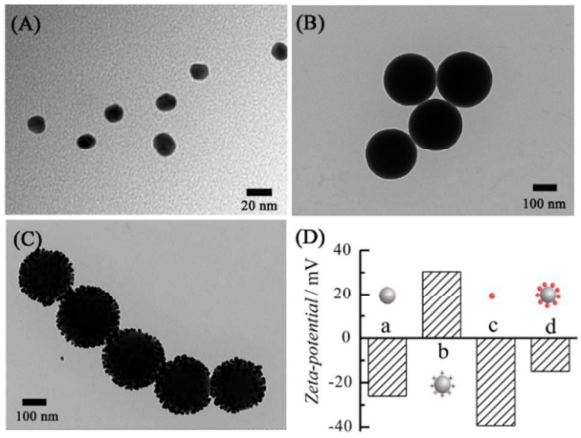

Fig. 1. TEM images of AuNPs(A), SiO_2 (B), SiO_2@AuNPs (C) and Zeta potentials histograms of (a) bare SiO_2, (b) amino-functionalized SiO_2, (c) AuNPs, and (d) SiO_2@AuNPs.

In addition, differential pulse voltammetric (DPV) measurement and electrochemical impedance spectroscopy (EIS) were carried out to investigate the interface engineering of the biocathode. Compared to that of 144.07 μA for the bare ITO electrode (Fig. 2A, curve b), the current value of $[Fe(CN)_6]^{3-}$ at the AuNPs-modified ITO electrode increased to about 149.73 μA (Fig. 2A, curve a), due to the efficient electron transport of AuNPs. After the peptide and MCH were modified on the electrode surface, the reduction currents of $[Fe(CN)_6]^{3-}$ showed a slight decrease in sequence (curve c, d, in Fig. 2A), suggesting that the small molecular almost have no effect on the electron transfer of $[Fe(CN)_6]^{3-}$. It should be noted that the current was still nearly no change (curve e) when SiO_2@AuNPs was added in the detected system in the absence of PKA, which suggested that only the bonded SiO_2@AuNPs on the peptide chain could play the role of blocking. However, when the peptide was thiophosphorylated in the presence of PKA, the SiO_2@AuNPs functionalized biocathode showed a significantly decreased current of 110.44 μA (curve f in Fig. 2A), which could be ascribed to the blocking effects and electrostatic repulsion of SiO_2@AuNPs composite bonded at peptide chain. Moreover, the results were also confirmed by EIS measurement. With the successive modification on the electrode surface, the charge-transfer resistance (R_{ct}) changed (Fig. 2B). As expected, only the bonded SiO_2@AuNPs showed

View Article Online
DOI: 10.1039/C8CC02328J

an elevated R_{ct}. Therefore, the obvious variation of the cathodic current and EIS signal with or without PKA indicated that the functionalized biocathode could be applied in the fabrication of the self-powered biosensor.

Under the above optimal experimental conditions, the relationship between the DPV response of the biocathode and PKA concentration was measured. As shown in Fig. S2, the reduction current of $[Fe(CN)_6]^{3-}$ decreased with the PKA concentration increasing from 0.0005 to 20 U mL^{-1}. This target-induced signal response laid a solid foundation for PKA detection and quantification and confirmed the feasibility for the as-proposed biosensor based on the interface engineering of the biocathode.

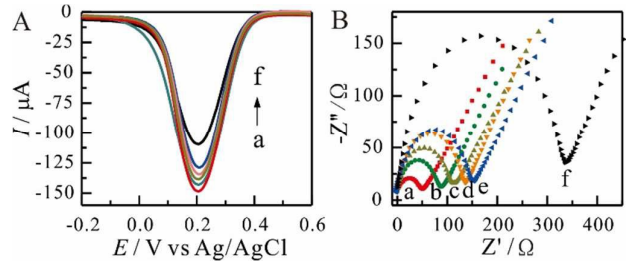

Fig. 2. DPV curves (A) and EIS curves (B) of AuNPs/ITO electrode (a), the bare ITO electrode (b), peptide/AuNPs/ITO electrode (c), MCH/peptide/AuNPs/ITO electrode (d), SiO_2@AuNPs-MCH/peptide/AuNPs/biocathode (e), and SiO_2@AuNPs-thiophosphorylated peptide/MCH/peptide/AuNPs/biocathode (f).

As the electron generator, the bioanode of the EBFC also plays a vital role in the construction of the self-powered biosensor. Herein, the NAD^+-dependent GDH modified CNT bioanode was fabricated to oxidize the glucose. First, EIS was used to characterize the assembly processes of the bioanode. As depicted in Fig. S3, due to the excellent conductivity of CNT, the R_{ct} of the $[Fe(CN)_6]^{3-/4-}$ probe decreased with CNT modification (curve b, 35 Ω) compared to that of the bare CP electrode (curve a, 141 Ω). After the assembly of GDH, the R_{ct} value obviously increased (curve c, 243 Ω), indicating the successful modification of GDH. To reduce the overpotential of NADH oxidation, the carboxyl modified CNT with good conductivity was used. As shown in Fig. S3B, the onset potential of NADH was approximately at -0.05 V, which demonstrated that the ability of CNT to reduce the overpotential of NADH oxidation. Furthermore, with the increasing of NADH concentration, the oxidation current was increased, which substantially suggested that the cofactor NAD^+ could be efficiently recycled through the electrocatalysis of CNT. In this case, the glucose oxidation of the GDH/CNT bioanode would be occurred. With the glucose addition, the oxidation current intensity increased, implying the efficient glucose oxidation at the GDH/CNT bioanode (Fig. S3C). All the above results from the bioanode and the biocathode measurements further confirmed the feasibility of the as-proposed self-powered biosensors.

On the basis of peptide/AuNPs/biocathode and GDH/CNT bioanode, the EBFC-based self-powered biosensing platform for PKA analysis was constructed. The PKA activity was evaluated with different concentrations of PKA. As shown in Fig. 3A, initially, the E^{OCV} of the as-proposed biosensor was about 0.6 V (curve a). When the target PKA was added, the E^{OCV} of the biosensor was negatively correlated with the PKA concentration (curves b-l). Furthermore, a linear relationship was presented between E^{OCV} and the logarithm of PKA concentration in the range from 0.0005 to 20 U mL^{-1} (Fig. 3B). The linear equation was E^{OCV}=0.455-0.040logc_{PKA}, and the coefficient of determination (R^2) was 0.9993. The detection limit of PKA was 0.00022 U mL^{-1} (S/N = 3), which exhibited comparable or superior performance in comparison with those of the reported methods (Table S1). It should be noted that the power output values of the biofuel cell decreased with the increasing of the PKA concentrations (Fig. S4). Therefore, under closed circuit mode, the design of the sensing properties could also be realized. However, to simplify the biosensing instrumentation (only a voltmeter needed), the E^{OCV} was selected as the signal response.

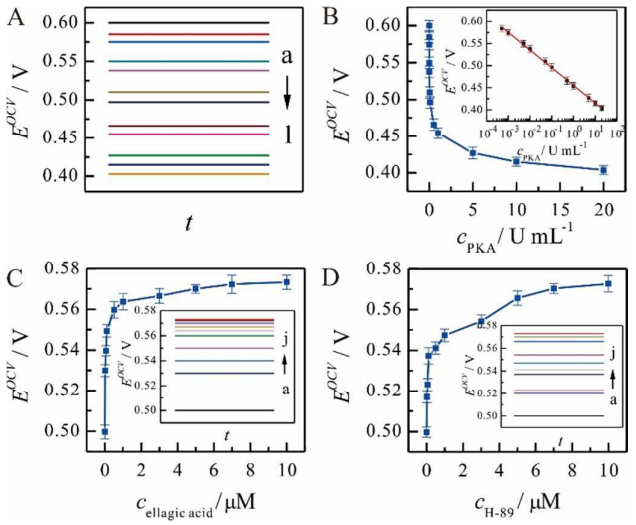

Fig. 3 (A) E^{OCV} signal under different PKA concentrations (a-l: 0, 0.0005, 0.001, 0.005, 0.01, 0.05, 0.1, 0.5, 1, 5, 10, 20 U mL^{-1}). (B) Variation of the E^{OCV} as a function of PKA concentration. The inset is the linear relationship between E^{OCV} and the logarithm value of PKA concentration. E^{OCV} of the self-powered biosensor in the presence of different concentrations of ellagic acid (C) and H-89 (D) (a-j: 0 0.01, 0.05, 0.10, 0.50, 1.00, 3.00, 5.00, 7.00, 10.00 μM). The concentrations of PKA and ATP-s are 0.1 U mL^{-1} and 50 μM, respectively.

In this case, the as-proposed approach was further applied in PKA inhibition assay, and the potent and cell-permeable inhibitor ellagic acid and H-89 were chosen as the models. As presented in Fig. S5A and S5B, the DPV signal of the biocathode significantly increased with the increase of inhibitors concentration, suggesting that the PKA activity was efficiently inhibited and the peptide thiophosphorylation level was lowered by inhibitions. As a consequence, the E^{OCV} values of the self-powered biosensors enhanced with the increase of the inhibitions concentration from 0.01 to 10 μM (Fig. 3C and 3D). The above results confirmed that the proposed detection strategy also had great potential in protein kinase inhibitor screening and drug discovery.

To deeply validate the practical application of this method in complex biological matrix analysis, we exploited the cell

View Article Online
DOI: 10.1039/C8CC02328J

lysates extracted from tumor cells (MCF-7 and A549). As seen in Table S2, the PKA concentration in tumor cell MCF-7 and A549 was 0.019 U mL^{-1} and 0.013 U mL^{-1}, respectively. The recoveries of 93.9-107.7% were achieved, demonstrating that the strategy showed a great promise to detect PKA activity in complex biological samples with excellent reliability.

Conclusions

In summary, a facile and ultrasensitive EBFC-based self-powered biosensing of protein kinase activity and inhibition was proposed via thiophosphorylation-mediated interface engineering. In this design, The steric hindrance and electrostatic repulsion of SiO_2@AuNPs composite could precisely control the diffusion of $[Fe(CN)_6]^{3-}$ on the interface of biocathode. In addition, the as-proposed biosensor also showed a low detection limit of 0.00022 U mL^{-1} (S/N = 3) and wide linear range (0.0005 to 20 U mL^{-1}) for PKA activity, comparable or superior to those of the reported methods. Thus, the as-proposed biosensing platform needs no external power sources and is featured with high sensitivity, simple instrumentation (only two electrodes necessary) and low cost. Meanwhile, it also exhibited excellent performance even in complicated biological samples and inhibitor screening. Therefore, this robust biosensor holds great potential in the applications of protein kinases-related clinic diagnostic and drug discovery.

We gratefully appreciate the financial support from the National Natural Science Foundation of China (21605092 and 21575074), the Natural Science Foundation of Shandong Province, China (ZR2016BQ08), the Basic Research Program of Qingdao (17-1-1-36-jch), the Research Foundation for Distinguished Scholars of Qingdao Agricultural University (663-1117002), and the Special Foundation for Distinguished Taishan Scholar of Shandong Province (ts201511052).

Conflicts of interest

There are no conflicts of interest to declare.

Notes and references

1. E. Katz, A. F. Bückmann and I. Willner, J. Am. Chem. Soc., 2001, 123, 10752-10753.
2. M. Zhou and J. Wang, Electroanalysis, 2012, 24, 197-209.
3. M. Zhou, Electroanalysis, 2015, 27, 1786-1810.
4. D. Majdecka, S. Draminska, D. Janusek, P. Krysinski and R. Bilewicz, Biosens. Bioelectron., 2018, 102, 383-388.
5. D. P. Hickey, R. C. Reid, R. D. Milton and S. D. Minteer, Biosens. Bioelectron., 2016, 77, 26-31.
6. C. Hou, S. Fan, Q. Lang and A. Liu, Anal. Chem., 2015, 87, 3382-3387.
7. P. P. Gai, C. C. Gu, T. Hou and F. Li, Anal. Chem., 2017, 89, 2163-2169.
8. C. C. Gu, P. P. Gai, T. Hou, H. Li, C. H. Xue and F. Li, ACS Appl. Mater. Interfaces, 2017, 9, 35721-35728.
9. J. Cheng, Y. Han, L. Deng and S. Guo, Anal. Chem., 2014, 86, 11782-11788.
10. M. Zhou, N. Zhou, F.Kuralay, J. R. Windmiller, S. Parkhomovsky, G. Valds-Ramrez, E. Katz and J. Wang., Angew. Chem., 2012, 124, 2740-2743.
11. P. P. Gai, R. B. Song, C. Zhu, Y. Ji, W. Wang, J. R. Zhang and J. J. Zhu, Chem. Commun., 2015, 51, 16763-16766.
12. P. P. Gai, Y. S. Ji, W. J. Wang, R. B. Song, C. Zhu, Y. Chen, J. R. Zhang and J. J. Zhu, Nano Energy, 2016, 19, 541-549.
13. F. Wu, P. Yu and L. Mao, Chem. Soc. Rev., 2017, 46, 2692-2704.
14. M. Grattieri and S. D. Minteer, ACS Sens., 2018, 3, 44-53.
15. D. Wen, L. Deng, S. Guo and S. Dong, Anal. Chem., 2011, 83, 3968-3972.
16. M. Zhou, Y. Du, C. Chen, B. Li, D. Wen, S. Dong and E. Wang, J. Am. Chem. Soc., 2010, 132, 2172-2174.
17. L. L. Wang, H. H. Shao, W. J. Wang, J. R. Zhang and J. J. Zhu, Nano Energy, 2017, 44, 95-102.
18. M. Zhou, F. Kuralay, J. R. Windmiller and J. Wang, Chem. Commun., 2012, 48, 3815-3817.
19. G. Manning, D. B. Whyte, R. Martinez, T. Hunter and S. Sudarsanam., Science, 2002, 298, 1912-1934.
20. P. Cohen, Nat. Cell Biol., 2002, 4 E127-E130.
21. M. E. M. E. Noble, J. A.; Johnson, L. N., Science, 2004, 303, 1800-1805.
22. M. Vieth, J. J. Sutherland, D. H. Robertson and R. M. Campbell, Drug Discovery Today, 2005, 10, 839-846.
23. Z. Wang, N. Sun, Y. He, Y. Liu and J. Li, Anal. Chem., 2014, 86, 6153-6159.
24. T. Skorski, Nat. Rev. Cancer, 2002, 2, 351-360.
25. H. F. Zhao, R. P. Liang, J. W. Wang and J. D. Qiu, Chem. Commun., 2015, 51, 12669-12672.
26. S. Xu, Y. Liu, T. Wang and J. Li., Anal. Chem., 2010, 82, 9566-9572.
27. M. J. Knape, L. G. Ahuja, D. Bertinetti, N. C. Burghardt, B. Zimmermann, S. S. Taylor and F. W. Herberg, ACS Chem. Biol., 2015, 10, 2303-2315.
28. T. Yoshida, M. Sato, T. Ozawa and Y. Umezawa., Anal. Chem., 2000, 72, 6-11.
29. Y. P. Kim, E. Oh, Y. H. Oh, D. W. Moon, T. G. Lee and H. S. Kim, Angew. Chem. Int. Ed. , 2007, 46, 6816-6819.
30. Z. Deng, M. Ye, Y. Bian, Z. Liu, F. Liu, C. Wang, H. Qin and H. Zou, Chem. Commun., 2014, 50, 13960-13962.
31. L. Zhang, W. Song, R. P. Liang and J. D. Qiu, Anal. Chem., 2016, 88, 11460-11467.
32. J. Zhou, X. Xu, W. Liu, X. Liu, Z. Nie, M. Qing, L. Nie and S. Yao, Anal. Chem., 2013, 85, 5746-5754.
33. Y. Xu, W. Shi, X. He, X. Wu, X. Li and H. Ma, Anal. Chem., 2017, 89, 10980-10984.
34. Y. Zhou, H. Yin, X. Li, Z. Li, S. Ai and H. Lin, Biosens. Bioelectron., 2016, 86, 508-515.
35. H. Yin, M. Wang, B. Li, Z. Yang, Y. Zhou and S. Ai, Biosens. Bioelectron., 2015, 63, 26-32.
36. I. S. Shin, R. Chand, S. W. Lee, H. W. Rhee, Y. S. Kim and J. I. Hong, Anal. Chem., 2014, 86, 10992-10995.
37. X. Xu, Z. Nie, J. Chen, Y. Fu, W. Li, Q. Shen and S. Yao, Chem. Commun., 2009, 6946-6948.
38. J. Liu, H. Cheng, D. He, X. He, K. Wang, Q. Liu, S. Zhao and X. Yang, Anal. Chem., 2017, 89, 9062-9068.
39. X. Li, L. Zhu, Y. Zhou, H. Yin and S. Ai, Anal. Chem., 2017, 89, 2369-2376.
40. Z. Yan, Z. Wang, Z. Miao and Y. Liu, Anal. Chem., 2016, 88, 922-929.

View Article Online
DOI: 10.1039/C8CC02328J

Enzymatic Biofuel Cell-Based Self-Powered Biosensing of Protein Kinase Activity and Inhibition via Thiophosphorylation-Mediated Interface Engineering

Chengcheng Gu[‡a], Panpan Gai[‡a], Lei Han[a], Wen Yu[a], Qingyun Liu[b] and Feng Li[*a]

[a] *College of Chemistry and Pharmaceutical Sciences, Qingdao Agricultural University, Qingdao 266109, P. R. China.*

[b] *College of Chemical and Environmental Engineering, Shandong University of Science and Technology, Qingdao 266510, P. R. China.*

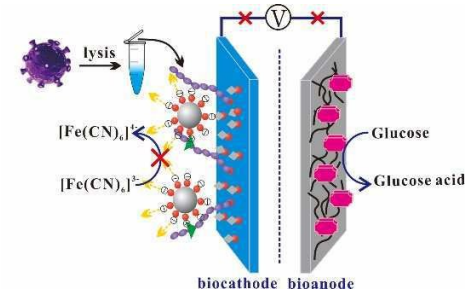

We developed a facile and ultrasensitive EBFC-based self-powered biosensing of protein kinase A activity and inhibition via thiophosphorylation-mediated interface engineering.

‡C. C. Gu & P. P. Gai contributed equally to this work.

* Corresponding author. E-mail: lifeng@qust.edu.cn; Tel/Fax: +86-532-86080855